

# Toward large-scale nonvolatile electrical programmable photonics with deterministic multilevel operation

Rui Chen<sup>1\*</sup>, Virat Tara<sup>1</sup>, Jayita Duta<sup>1</sup>, Minhoo Choi<sup>1</sup>, Justin Sim<sup>1</sup>, Julian Ye<sup>2</sup>, Jiajiu Zheng<sup>1</sup>, Zhuoran Fang<sup>1</sup>, and Arka Majumdar<sup>1,2\*</sup>

<sup>1</sup>Department of Electrical and Computer Engineering, University of Washington, WA, USA

<sup>2</sup>Department of Physics, University of Washington, WA, USA)

\*[charey@uw.edu](mailto:charey@uw.edu), [arka@uw.edu](mailto:arka@uw.edu)

**Abstract:** We present a deterministic multi-level scheme by electrically controlling multiple phase-change material (PCM)  $\text{Sb}_2\text{S}_3$  segments through individual PIN heaters. PCMs are integrated on 300-mm silicon photonic fab dies back-end-of-line, promising for fast-prototyping and massive production. © 2024 The Author(s)

## 1. Introduction

Programmable photonic integrated circuits (PICs) [1] can realize different functionalities through reconfiguring on-chip photonic components and are at the heart of modern photonic technologies. Among many tuning techniques, phase-change materials (PCM) [2–5] have gained much attention due to their unique nonvolatile nature, meaning zero static energy consumption after switching the devices and hence a truly “set-and-forget” operation. While optically actuated PCM photonic systems have been used for in-memory optical computing up to a scale of  $8 \times 8$  [6], no large-scale electrically controlled systems have been shown, despite of its promise for a much faster, more accessible real-time system control. This can be primarily attributed to the unavailability of the PCMs in the current silicon photonic foundries. Most of the hybrid PCM silicon photonic circuits are fabricated in-house, where the more complicated fabrication procedure, such as doping and metallization, leads to a lower success rate, hence a prolonged designing and testing cycle. One solution is to rely on foundries for technologically mature silicon photonic processes and to only focus on integration of PCMs in-house.

In this work, we demonstrated a fast-prototyping approach, where we took advantage of the mature 300-mm silicon photonic fab to significantly simplify the in-house process – only PCM deposition and patterning were done in-house. To illustrate the versatility of this platform, we showed a wide range of electrically controlled PCM photonic devices, including micro-ring resonators (MRRs), Mach-Zehnder interferometers (MZIs), and asymmetric directional couplers (DCs). We show that 25- $\mu\text{m}$ -long, 20-nm-thick  $\text{Sb}_2\text{S}_3$  can provide a large, reversible phase shift ( $\sim 0.3\pi$ ) in MRRs, and the loss due to the  $\text{Sb}_2\text{S}_3$  was only  $\sim 0.11$  dB. A cyclability test in an unbalanced MZI showed more than 500 switching events. Besides, to showcase the fast-prototyping advantage of this approach, we demonstrated a novel scheme to realize deterministic multilevel operation in DCs and MZIs using multiple ( $N$ )  $\text{Sb}_2\text{S}_3$  segments on a single device, individually controlled by  $N$  interleaved PIN diode heaters. We further achieved  $2^N$  levels by engineering the lengths of the  $\text{Sb}_2\text{S}_3$  segments to a geometric sequence with a common ratio of 2. This work shows a crucial step toward extremely large-scale programmable PCM-PICs with electrical control.

## 2. Results

Fig. 1a shows a 300-mm pure silicon photonic wafer, which was fabricated in a 300-mm semiconductor fab. We then opened the oxide window ( $\sim 5$   $\mu\text{m}$  wide) on the silicon waveguides through a hybrid dry-wet etching process to reduce the wet etch undercut. Lastly, we deposited and patterned 20-nm thick low-loss PCM  $\text{Sb}_2\text{S}_3$  in-house via a liftoff process using bilayer PMMA(MMA)/PMMA resist (Fig. 1b). We note the PCM integration process is at the back end of a 300-mm fab line, and no change is required on the 300-mm fab process.

We first demonstrate that diverse types of programmable components can be realized in this platform, including micro-ring resonators (MRRs) and Mach-Zehnder Interferometers (MZIs). Fig. 1c shows four reversible switching cycles of a nonvolatile tunable MRR with 25- $\mu\text{m}$ -long  $\text{Sb}_2\text{S}_3$ . The PIN diode has a resistance of around 62.5  $\Omega$  and a turn on voltage of around 0.9 V for this device. The electric pulse conditions are listed in the figure caption, and a resonance shift of around 0.4 nm is observed. The free spectral range (FSR) of this MRR is around 2.7 nm, and we estimate a phase shift of  $\sim 0.3\pi$ . By fitting the ring’s spectrum to a Lorentz line shape, we extract a quality factor of 55500 (37500) for amorphous (crystalline)  $\text{Sb}_2\text{S}_3$ . Therefore, the loss of crystalline  $\text{Sb}_2\text{S}_3$  is extracted as 0.11 dB, i.e., loss per  $\pi$  is around 0.4 dB. We note that this resonance shift is smaller compared to recently reported results [7] due to differences in the waveguide geometry. In Fig. 1d, we present a reversible switching result for an unbalanced MZI with 60- $\mu\text{m}$ -long  $\text{Sb}_2\text{S}_3$ . The resonance shift was only around 1 nm for an FSR of  $\sim 8$  nm. The extracted phase shift was  $\sim 0.25\pi$ , which leads to a smaller phase shift per unit length compared

to the MRR. We attribute this to incomplete phase change and could be further improved by optimizing the metal pad geometry. Fig. 1e shows the cyclability test results for the same MZI device, where the device showed good contrast after more than 500 switching cycles. The shift in the transmission level is attributed to partial damage of the  $\text{Sb}_2\text{S}_3$  during the switching test, which again could be overcome in the future.

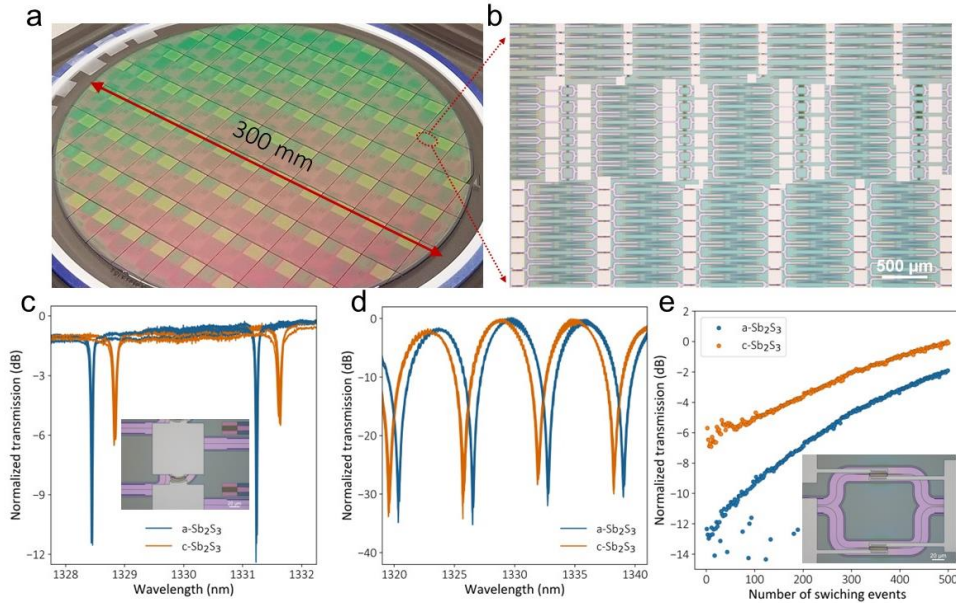


Fig. 1. A fast-prototyping platform for nonvolatile electrically controlled photonic integrated circuits by integrating PCMs at the backend-of-line of a 300-mm silicon photonic fab. (a) A photograph showing the 300-mm pure silicon photonic wafer. (b) Zoomed-in micrograph of a post-processed photonic die with metal wires and PCMs on it. (c) Reversibly tuning an MRR for 4 cycles by electrically switching 20-nm-thick, 25- $\mu\text{m}$ -long  $\text{Sb}_2\text{S}_3$  thin film on the intrinsic waveguide. Pulse conditions: 6.9 V, 500 ns for amorphization and 2.9 V, 200 ms for crystallization. (d) Reversibly tuning an MZI for 5 cycles by electrically switching 20-nm-thick, 60- $\mu\text{m}$ -long  $\text{Sb}_2\text{S}_3$  thin film on the intrinsic waveguide. Pulse conditions: 14.7 V, 500 ns for amorphization and 5.5 V, 200 ms for crystallization. (e) Alternatively sending in the amorphization/crystallization pulses to test the endurance of the device.

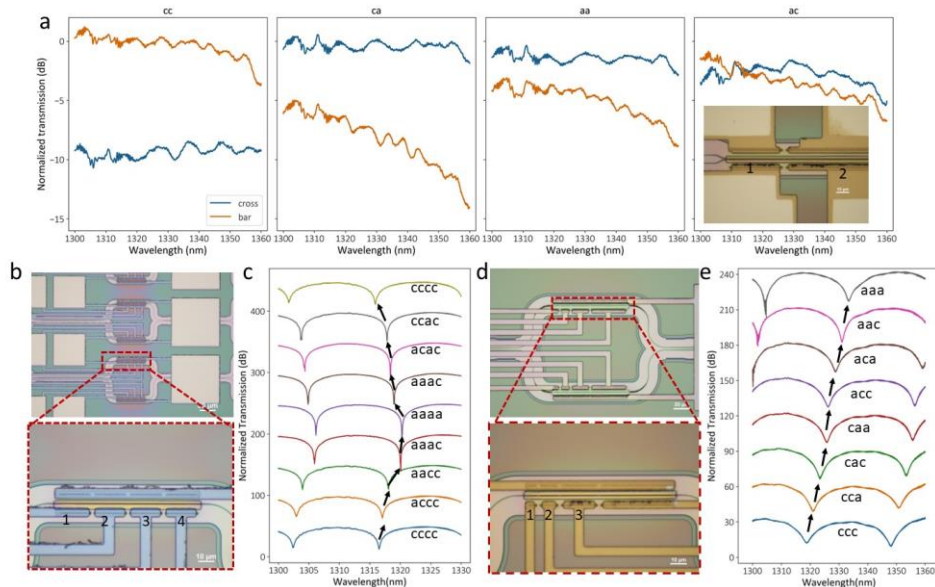


Fig. 2. Individually controlled  $\text{Sb}_2\text{S}_3$  segments for deterministic multilevel operation. (a) a multilevel directional coupler with two segments with unequal lengths can achieve cross, bar and intermediate levels. (b) Micrograph of 4-segment  $\text{Sb}_2\text{S}_3$  with equal length, which shows (c) 5 operation levels. Reversible switching is also demonstrated by bringing the system level back. The phase of the  $\text{Sb}_2\text{S}_3$  segments is indicated near each curve. (d) Micrograph of 4-segment  $\text{Sb}_2\text{S}_3$  with unequal length (only 3 segments were used). (e) Experimentally show that 8 ( $2^3$ ) operation levels can be achieved with the lengths of the segments in a geometric series with common ratio of 2. The spectrum is continuously shifted.

Next, we show a scheme to achieve deterministic multilevel operation, a challenging task for electrically switched PCMs [8]. We individually controlled multiple segments of  $\text{Sb}_2\text{S}_3$  thin films on silicon WGs using

interleaved PIN diode heaters. Each  $\text{Sb}_2\text{S}_3$  segment is switched electrically to either fully amorphous or crystalline phase, hence a deterministic operation. By programming the phase of each segment, multiple operation levels were obtained. We note that this idea of using multiple segments of PCMs has been shown recently in other works, but with a different PCM GSSe and tungsten heaters [9]. However, the demonstration was limited to pure amplitude modulation and here we show phase-only modulation with the low-loss PCM  $\text{Sb}_2\text{S}_3$  in DCs and MZIs. Multilevel directional couplers (DCs) are demonstrated in Figs. 2a. The inset in the last figure shows the micrograph of the device. This directional coupler has two actively tunable  $\text{Sb}_2\text{S}_3$  segments – the longer one (segment 2) is for cross/bar tuning and the shorter one (segment 1) can switch the DC to roughly 50:50 splitting ratio. We then extend to 4 segments to provide more operation levels in an unbalanced MZI as shown in Figs. 2b. Here, each segment has the same length and by changing the number of amorphous/crystalline segments, at most 5 levels could be achieved. Fig. 2c shows the experimental results, where we achieved 5 operation levels and demonstrated reversible switching between levels. As one step further, we experimentally show that  $N$   $\text{Sb}_2\text{S}_3$  segments could render  $2^N$  levels by engineering the lengths of segments as a geometric sequence with common ratio of 2, as shown in Fig. 2d. Here we only use 3 segments out of 4 to illustrate the idea. We denote the length of  $\text{Sb}_2\text{S}_3$  segment  $i$  as  $L_i$ , then  $L_1:L_2:L_3=1:2:4$ , since the phase modulation is proportional to the length, the phase shift induced by each segment has the same ratio  $\phi_1:\phi_2:\phi_3=1:2:4$ . We experimentally show that by different combination of the segments' phases, 8 ( $2^3$ ) distinct levels can be achieved. This exponential increase in the number of levels is critical to reduce the complexity of the control circuits and for large-scale integration.

### 3. Discussion

In conclusion, we have demonstrated a fast-prototyping platform to create nonvolatile programmable PICs. The massively produced silicon photonic chips from a 300-mm fab contained all the necessary components, such as grating couplers, power splitters, doping regions, and layer connect vias, which significantly simplified the in-house fabrication and could potentially facilitate testing different PCMs. MRRs, MZIs and DCs were designed and tested on this platform. Moreover, we showed deterministic multi-level operation via interleaved PIN diode heaters that individually control  $\text{Sb}_2\text{S}_3$  segments.  $2^N$  levels were achieved by engineering the length of each  $\text{Sb}_2\text{S}_3$  segment. Our work shows a crucial step to facilitate the research in PCMs and to push the PCM tunable PICs toward large scales.

### Acknowledgements

The authors would like to acknowledge Intel Corp. for fabrication of the silicon photonics wafers and thank John Heck, Harel Frish, Haisheng Rong for useful discussions. The research is funded by National Science Foundation (NSF-1640986, NSF-2003509), ONR-YIP Award, DARPA-YFA Award, NASA-STTR Award 80NSSC22PA980, and Intel. Part of this work was conducted at the Washington Nanofabrication Facility/ Molecular Analysis Facility, a National Nanotechnology Coordinated Infrastructure (NNCI) site at the University of Washington, with partial support from the National Science Foundation via awards NNCI-1542101 and NNCI-2025489. Part of this work was performed at the Stanford Nano Shared Facilities (SNSF), supported by the National Science Foundation under award ECCS-1542152).

### References

- [1] W. Bogaerts, D. Pérez, J. Capmany, D. A. B. Miller, J. Poon, D. Englund, F. Morichetti, and A. Melloni, "Programmable photonic circuits," *Nature* **586**, 207–216 (2020).
- [2] S. Abdollahramezani, O. Hemmatyar, H. Taghinejad, A. Krasnok, Y. Kiarashinejad, M. Zandehshahvar, A. Alù, and A. Adibi, "Tunable nanophotonics enabled by chalcogenide phase-change materials," *Nanophotonics* **9**, 1189–1241 (2020).
- [3] N. Youngblood, C. A. Ríos Ocampo, W. H. P. Pernice, and H. Bhaskaran, "Integrated optical memristors," *Nat. Photon.* **17**, 561–572 (2023).
- [4] Z. Fang, R. Chen, J. Zheng, and A. Majumdar, "Non-Volatile Reconfigurable Silicon Photonics Based on Phase-Change Materials," *IEEE JSTQE* **28**, 8200317 (2022).
- [5] R. Chen, Z. Fang, F. Miller, H. Rarick, J. E. Fröch, and A. Majumdar, "Opportunities and Challenges for Large-Scale Phase-Change Material Integrated Electro-Photonics," *ACS Photon.* **9**, 3181–3195 (2022).
- [6] J. Feldmann, N. Youngblood, M. Karpov, H. Gehring, X. Li, M. L. Gallo, X. Fu, A. Lukashchuk, A. S. Raja, et al., "Parallel convolution processing using an integrated photonic tensor core," *Nature* **589**, 52–58 (2020).
- [7] R. Chen, Z. Fang, C. Perez, F. Miller, K. Kumari, A. Saxena, J. Zheng, S. J. Geiger, K. E. Goodson, et al., "Non-volatile electrically programmable integrated photonics with a 5-bit operation," *Nat. Comm.* **14**, 3465 (2023).
- [8] T. Tuma, A. Pantazi, M. Le Gallo, A. Sebastian, and E. Eleftheriou, "Stochastic phase-change neurons," *Nat. Nanotechnol.* **11**, 693–699 (2016).
- [9] J. Meng, Y. Gui, B. M. Nouri, X. Ma, Y. Zhang, C.-C. Popescu, M. Kang, M. Miscuglio, N. Peserico, et al., "Electrical programmable multilevel nonvolatile photonic random-access memory," *Light Sci Appl* **12**, 189 (2023).